

ACCURATE EVALUATION OF BUILDING DAMAGE IN THE 2003 BOUMERDES, ALGERIA EARTHQUAKE FROM QUICKBIRD SATELLITE IMAGES

ABDELGHANI MESLEM*

*Department of Urban Environment Systems
Graduate School of Engineering, Chiba University
1-33 Yayoi-cyo, Inage-ku, Chiba 263-8522, Japan*

FUMIO YAMAZAKI and YOSHIHISA MARUYAMA

*Graduate School of Engineering, Chiba University
1-33 Yayoi-cyo, Inage-ku, Chiba 263-8522, Japan*

Accepted 8 October 2010

Using QuickBird satellite images of Boumerdes city obtained following the 21 May 2003 Algeria earthquake, our study examined the applicability of high-resolution optical imagery for the visual detection of building damage grade based on the ground-truth data on the urban nature, typology of a total of 2,794 buildings, and the real damage observed. The results are presented as geographical information system (GIS) damage mapping of buildings obtained from field surveys and QuickBird images. In general, totally collapsed buildings, partially collapsed buildings, and buildings surrounded by debris can be identified by using only post-event pan-sharpened images. However, due to the nature of the damage observed, some buildings may be judged incorrectly even if pre-event images are employed as a reference to evaluate the damage status. Hence, in this study, we clarify the limitations regarding the applicability of high-resolution optical satellite imagery in building damage-level mapping.

Keywords: QuickBird; satellite image; damage detection; the 2003 Algeria earthquake.

1. Introduction

It is very important for emergency management and recovery/restoration planning to estimate the damage distribution immediately after an earthquake or other disasters. To obtain damage data from affected areas, field investigation is the most common and most reliable option [Goretti and Pasquale, 2004; Hisada *et al.*, 2004]. After the 1999 Kocaeli earthquake in Turkey, the Architectural Institute of Japan *et al.* [2001] carried out damage survey in the affected area and the database for more than 2,700 buildings was constructed. Earthquake Engineering Research Institute recently compiled the reconnaissance forms of field investigations for earthquake disasters in the world [EERI, 2009]. Field surveys, however, take long time if the target area is large and damages are widely distributed.

*Corresponding author.

Recent advancements in remote sensing technologies and its applications have made it possible to use remotely sensed imagery for estimating the damage distribution due to natural disasters [Yamazaki and Matsuoka, 2007; Rathje and Adams, 2008; Eguchi *et al.*, 2008]. Among them, high-resolution optical satellite imagery, which has become available in the last decade, made satellite remote sensing more useful in disaster management since even the damage status of individual buildings can be identified without visiting the sites of disasters. The high-resolution satellite images obtained by Ikonos, QuickBird, and more recently, GeoEye-1 and WorldView-1 & -2 have been used widely to assess the damages due to recent natural disasters.

Ikonos is the first civilian high-resolution optical satellite with maximum spatial resolution of 1.0 m, in operation since 1999. It captured a clear image of Bhuj area after the 26 January 2001 Gujarat, India earthquake. Saito *et al.* [2004] performed visual damage inspection using the post-event Ikonos image and pre-event other satellite images. After this event, Ikonos captured many pre- and post-event images of disaster-affected areas [Chiroiu *et al.*, 2005].

QuickBird, the most widely used high-resolution optical satellite with the maximum spatial resolution of 0.6 m, has been in operation since 2001. The first pre- and post-event image pair were taken for the 21 May 2003 Boumerdes, Algeria earthquake and they were used in assessing damage detection [Yamazaki *et al.*, 2004]. QuickBird images were also used to detect damage areas from the 2003 Bam, Iran earthquake [Rathje *et al.*, 2005; Saito *et al.*, 2005; Yamazaki *et al.*, 2005], the 2006 Java, Indonesia earthquake [Yamazaki and Matsuoka, 2007], and many other disasters [Eguchi *et al.*, 2008].

However, due to the lack of detailed geographical information system (GIS) ground-truth data, the accuracy of damage detection for optical satellite imagery has not been analyzed in detail. Although results by visual inspection are often considered as a benchmark for automated image interpretation or change-detection analyses, visual inspection of satellite images has some limitation. In addition to the shortage of ground-truth data obtained from field surveys, the examination of the accuracy of identified or judged damage grades may also depend on the nature of existing buildings, urban structure, and the environment of the region. Shadow and vegetation were pointed out to affect detecting building damage in the 2003 Bam [Yamazaki *et al.*, 2005] and the 2006 Central Java earthquakes [Miura and Midorikawa, 2010].

In this paper, we present the results of visual damage grade interpretation using high-resolution satellite images for the 2003 Boumerdes, Algeria earthquake. Visual damage interpretation based on the European Macroseismic Scale (EMS-98) was carried out building-by-building through a comparison of pre- and post-event images. The estimation of damage grade was mainly based on geometry changes and debris. The results of the damage inspection were compared with field survey data, and the accuracy and usefulness of the high-resolution satellite images in

damage detection was demonstrated while considering both the building type and urban environment.

2. QuickBird Imagery in Response to the 2003 Algeria Earthquake

2.1. QuickBird imagery of boumerdes, Algeria

Following the 21 May 2003 Algeria earthquake [Meslem *et al.*, 2008], the QuickBird satellite was used to capture the impact of the earthquake in the Boumerdes city in the Boumerdes province, as shown in Fig. 1. These pan-sharpened images were produced by combining panchromatic images of 0.6 m resolution and multi-spectral images of 2.4 m resolution. These images, considered to be the first sets of clear images of an earthquake disaster acquired by a civilian high-resolution satellite, were taken about one year before (April 22, 2002) and two days after (May 23, 2003) the event, with different off-nadir view angles of 11.2° and 24.3° , respectively. Using these images, Yamazaki *et al.* [2004] performed visual damage detection for the Boumerdes city following the earthquake. However, the accuracy of the visual interpretation was examined only for the first stage due to the lack of detailed ground-truth data on the damage and characteristics of buildings.

Boumerdes city, the capital of the Boumerdes province, is located in north-central Algeria about 50 km east of Algiers and along the Mediterranean Sea

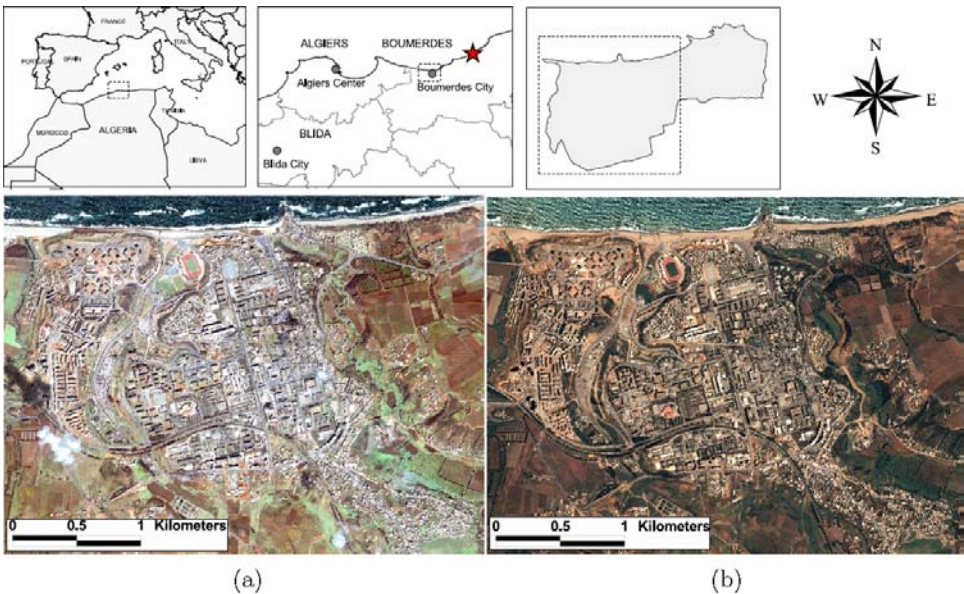


Fig. 1. Pan-sharpened natural color QuickBird satellite images of Boumerdes city captured before and after the 2003 Algeria earthquake: (a) the preevent image captured on June 22, 2002 (before 394 days) and (b) the post-event image captured on May 23, 2003 (after two days). The red star represents the epicenter of the mainshock.

(Fig. 1). Its previous name before the independence of Algeria in 1962 was Rocher Noir, which means “black rock” in French. The city became the eponymous capital of its province in 1984, according to the administrative division. In 1998, the population was estimated to be 33,646. The urban area is concentrated on the western part of the administrative boundary of the city; and the eastern part is mainly used for agriculture. The QuickBird images presented in this study show only the urbanized area of Boumerdes city.

According to the database created from the data collected for this study, the total number of existing constructions in Boumerdes before the earthquake is estimated to be 2,794. As much as 43% (1,200) of the total constructions were modern buildings owned by the public for residential use, industrial or commercial activities, offices, education, etc. The buildings in this category have 1–10 stories. The remaining 57% (1,594) of the constructions in Boumerdes were privately owned houses for residential use, some of which housed commercial activities (shops) on the first story (ground story). The number of stories for existing houses ranged from 1 to 3 stories. Figure 2(a) shows an example of the post-earthquake view corresponding to the southwestern part of the city, where there are many modern medium-rise buildings. Figure 2(b) shows an example of the post-earthquake view of a densely built-up area. This image corresponds to the southeastern part of the city, where almost all of the existing constructions were single, nonengineered, 1–3 story private houses.

For this study, we divided the constructions into three classes according to height: low-rise (1–3 stories), which comprised 71% of the total (2001 constructions); medium-rise (4–6 stories), which comprised 25% (691 constructions), and high-rise (7+ stories), which comprised the remaining 4% (102 constructions). Figure 3 shows the GIS distribution by height classes of the 2,794 constructions in Boumerdes city before the earthquake.



Fig. 2. Post-event images of Boumerdes city: (a) an area of modern medium- to high-rise constructions and (b) a densely built area mostly with low-rise constructions.

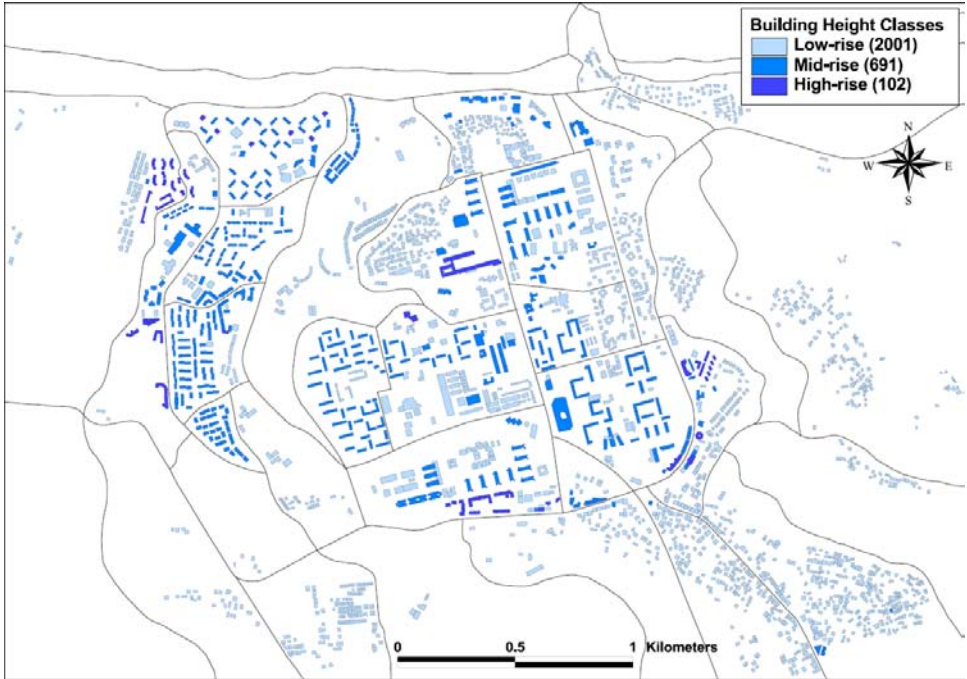












Fig. 3. Construction classification according to building height in Boumerdes city.

In terms of construction material, 92% of the total 2,794 constructions were RC structures built between 1969 and 2003; they consisted of columns and beams with unreinforced hollow bricks used as external and internal walls and with RC shear walls. The existing masonry constructions were built before 1962 and comprise only a small fraction (4%) of the total. There were very few constructions of steel or wood (2% and 1%, respectively), most of which were for industrial use.

2.2. Visual building damage grades detection and comparison with field survey

A field survey by engineers from the Algerian Ministry of Housing was started one week after the earthquake covering all the affected areas in the Boumerdes and Algiers provinces [Belazougui *et al.*, 2008; Meslem *et al.*, in press]. This field survey mission, which lasted until June 30, 2003, was conducted based on a scale of five damage grades [Meslem *et al.*, 2009] that was adopted by the Algerian National Centre of Earthquake Engineering (CGS); each grade corresponds very closely to the European Macroseismic Scale EMS-98 [Grünthal, 2001], as shown in Table 1. According to the EMS-98 scale, no and slight damage is classified as Grade 1, moderate damage as Grade 2, heavy damage as Grade 3, very heavy damage as Grade 4, and partial or total collapse as Grade 5.

Table 1. Damage grading for reinforced concrete and masonry buildings according to the European Macroseismic Scale [European Seismological Commission, 1998]. This damage grading corresponds to that used by CGS during the field survey following the 2003 earthquake.

Damage pattern		Description of damage level
Reinforced concrete	Masonry	
		Grade 1: No or negligible-to-slight damage to nonstructural elements, and no damage to structural elements
		Grade 2: Slight-to-moderate damage to nonstructural elements, and slight damage to structural elements
		Grade 3: Heavy damage to nonstructural elements, and moderate damage to structural elements
		Grade 4: Very heavy damage to nonstructural elements, and heavy damage to structural elements
		Grade 5: Very heavy structural damage, with part of the building collapsed, or total collapse.

Using both pre- and post-earthquake satellite images as shown in Fig. 1, visual detection of building damage grades was conducted based on the EMS-98 classification for comparison with real damage data from the field survey.

In general, for visual detection from vertical images, the damage can be detected by observing the absence or decrease of shadows, geometric irregularities of contours, and the heterogeneity of the roofs. Accordingly, totally collapsed buildings (Grade 5), partially collapsed buildings (Grade 4), and buildings surrounded by debris (Grade 3) can only be identified from post-event images. An example is shown in Fig. 4, where a building that is totally collapsed and surrounded by debris was easily detected.

Therefore, Grade 1, Grade 2, and some of Grade 3 structures cannot be detected from QuickBird images. This is because nonstructural damage (Table 1) cannot be identified from vertical images. However, some types of damage from Grade 3 can be detected and becomes easier for Grades 4 and 5. Accordingly, the damage judgments for grades of buildings were classified into four parts: Grade 1–2, Grade 3, Grade 4, and Grade 5.

Based on this visual interpretation using QuickBird images, the 2,794 buildings (including houses) were divided into groups of 2,526; 169; 35; and 64 for Grades 1 and 2; 3; 4; and 5, respectively. These results from satellite images were compared with ground-truth data from the field survey, which classified 2,258 buildings in Grades 1 and 2, 230 buildings in Grade 3, 243 buildings in Grade 4, and 63 buildings in Grade 5. We created two maps of GIS damage grade distributions for buildings

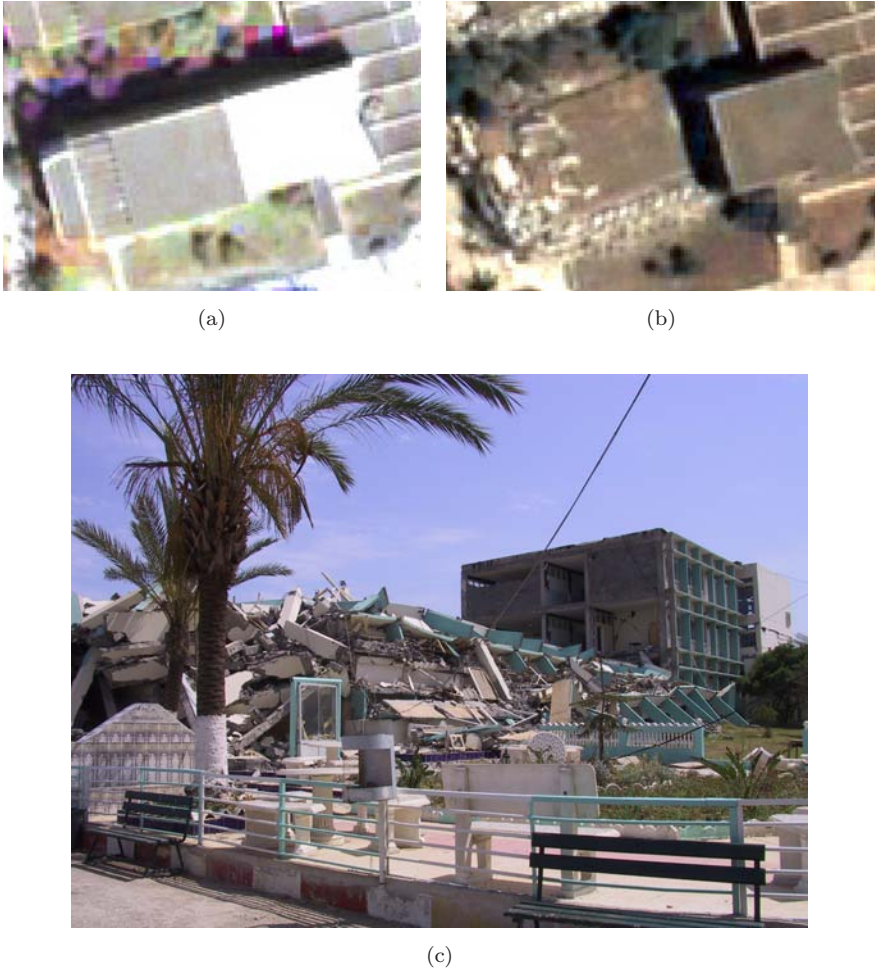
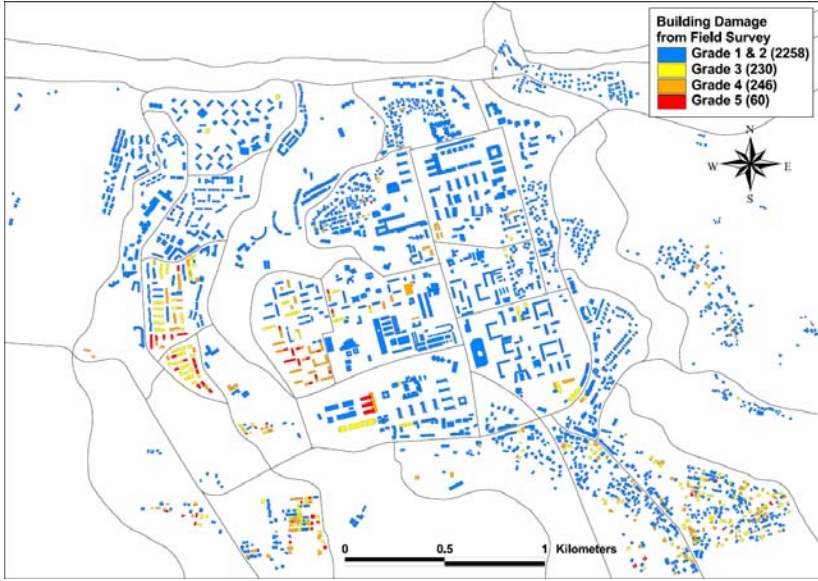


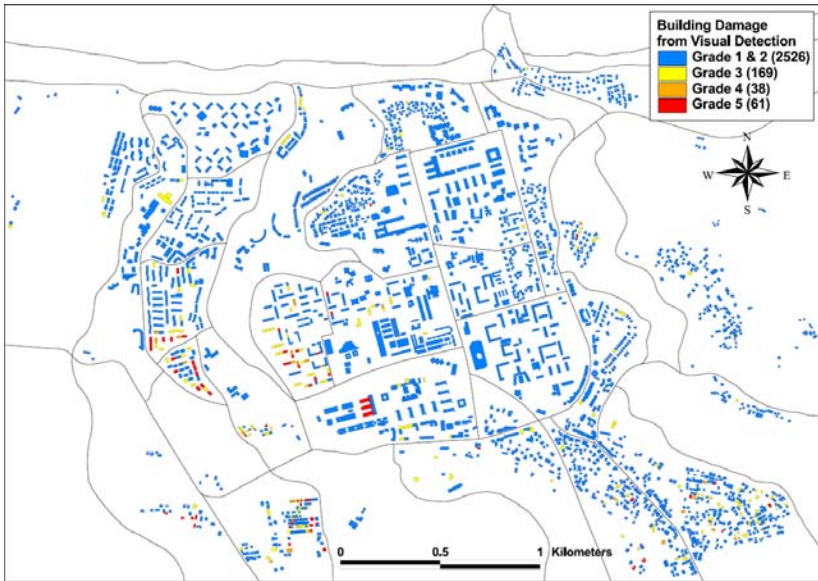
Fig. 4. Detection of a totally collapsed building: (a) the preevent QuickBird image, (b) the post-event QuickBird image, and (c) a photograph from the ground.

in Boumerdes city from two types of data: (a) from the field survey results and (b) from visual detection results using QuickBird images. Figure 5 shows a comparison of the two GIS damage maps.

By zone-level mapping, the visual detection results from the QuickBird images are shown to be clearly very close to the ground-truth data from the field survey. In building-level mapping, very heavy damage seems to be localized well from satellite images through visual detection. However, several buildings from the less severe part of Grade 3 were incorrectly judged by visual interpretation, as expected. Figures 6 and 7 show a comparison of damaged building ratios for very heavily damaged and collapsed (Grades 4 and 5) structures between the field survey result and the visual detection result from the satellite images. The damage ratios

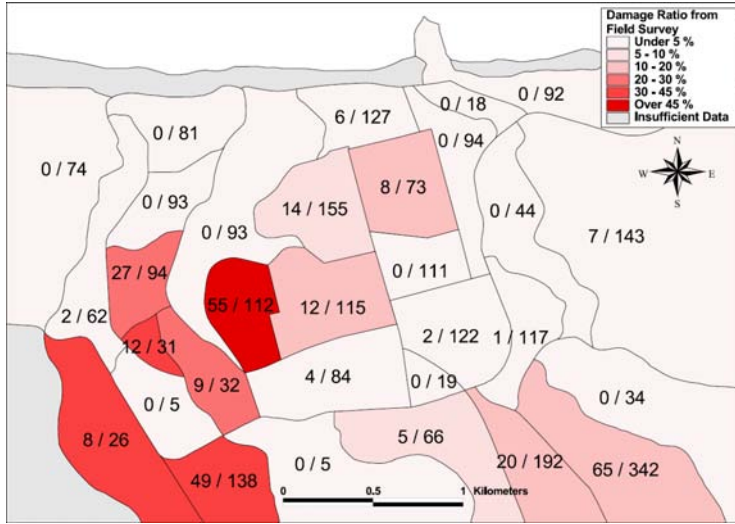


(a)

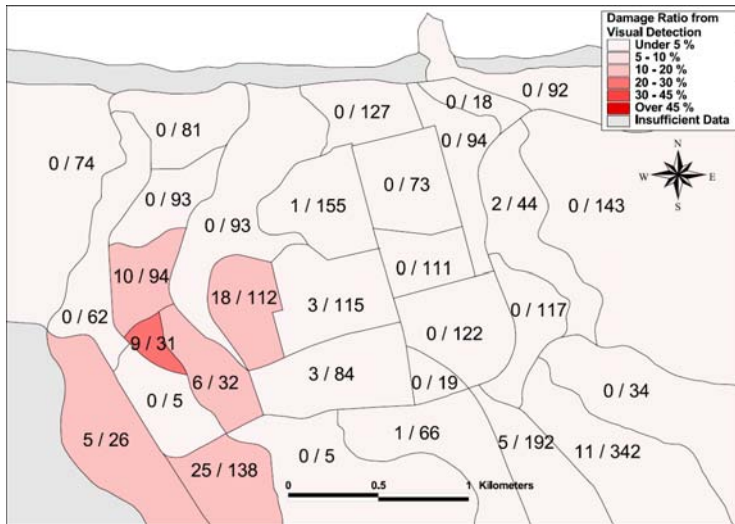


(b)

Fig. 5. Comparison of GIS damage distribution maps of existing buildings in Boumerdes after the 2003 Algeria earthquake: (a) the map obtained from field survey mission and (b) the map obtained from visual detection using the pre- and post-event QuickBird images.



(a)



(b)

Fig. 6. Building damage ratios of very heavily damaged and collapsed structures (Grades 4–5): (a) field survey results and (b) results of visual detection using the QuickBird images.

based on visual damage detection were underestimated compared with those based on the field survey. This is because some buildings suffering from Grade 4 damage were incorrectly judged by visual detection; this is in contrast to buildings suffering from Grade 5 damage, which generally corresponds to total or partial collapse.

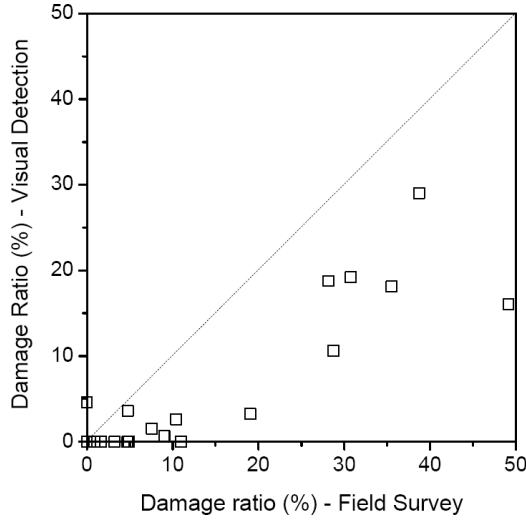
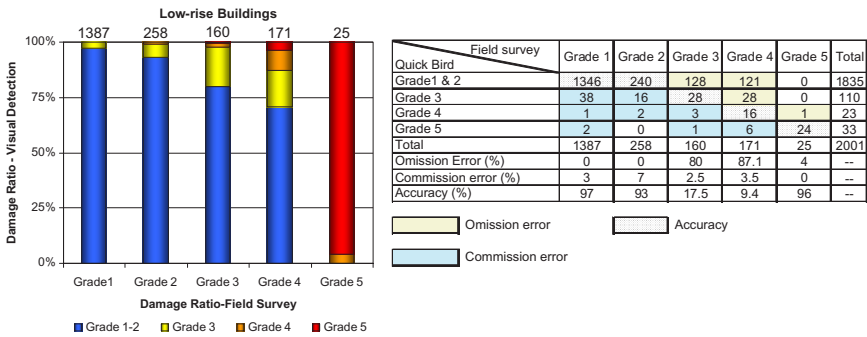
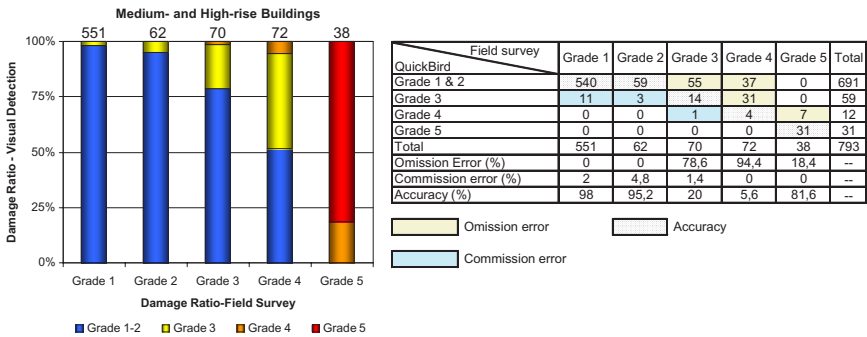


Fig. 7. Comparison of damage ratios computed using damage data from field survey with that computed using estimated damage data from the QuickBird satellite images by visual detection.



(a)



(b)

Fig. 8. Accuracy of distinguishing building damage grades from high-resolution satellite imagery by building height class: (a) Damage grade accuracy for low-rise buildings and (b) Damage grade accuracy for medium- and high-rise buildings.

3. Accuracy Analysis and Discussion

In general, for total collapses the damage is easily detectable. However, for low-rise construction, most are houses (small constructions) located in densely urban environments, as in Boumerdes city (Fig. 2(b)); sometimes, it is difficult to detect damage even when both pre- and post-event images are used. In such areas, it is not easy to observe decreases in shadow, debris surrounding a small damaged low-rise construction, etc. due to the urbanized conditions.

We examined the accuracy of using QuickBird images in detecting damage grades by considering the nature of urban environments and building height classes, as shown in Figs. 2 and 3. Figure 8 presents a comparison of damage grade detection



Fig. 9. A 4-story building that suffered from soft-story damage evaluated as Grade 4 from field survey; this structure was incorrectly judged as Grade 1-2 through visual detection from the QuickBird images: (a) the preevent QuickBird image, (b) the post-event QuickBird image, and (c) a photograph from the ground.

results in terms of building height classes for low-rise buildings and medium- and high-rise buildings.

For low-rise constructions located in densely built-up areas, most are houses built without any seismic code and evaluated as nonengineered structures [Meslem *et al.*, 2009]. Omission errors (judging damage grades as lower than the field survey result) become significant for Grades 3 and 4; out of 160 and 171 buildings identified by the field survey as Grades 3 and 4, respectively, only 28 (17.5%) and 16 (9.4%) buildings were judged as Grades 3 and 4, respectively, by visual damage detection. This observation shows that some amount of omission error should be expected and considered when estimating damage statistics from QuickBird images for lighter damage to low-rise constructions located in densely built-up areas. In contrast, commission errors (judging damage as higher grades than the field survey result) were shown to be not so significant for visual damage detection.



Fig. 10. Damage detection accuracy for a slightly tilted building: (a) the pre-event QuickBird image, (b) the post-event QuickBird image, and (c) a photograph from the ground.

Damage was extensively concentrated in the southwestern part of the city (Fig. 5), where there are many modern medium-rise buildings (Figs. 2(a) and 3); this explains why the damage ratio is more important for medium-rise buildings evaluated as engineered structures. Figure 8 clearly shows that some of these medium-rise buildings that suffered from Grades 3 and 4 damages were incorrectly judged by visual detection through QuickBird images. The omission error was estimated to be 79% and 94% for the detection of Grades 3 and 4, respectively; out of 70 and 72 medium-rise buildings identified by the field survey as Grades 3 and 4, respectively, only 14 (20%) and 4 (5.6%) medium-rise buildings were judged to be so by visual damage detection.

Figure 9 shows an example of a 4-story building suffering from soft-story damage classified as Grade 4 by the field survey and incorrectly judged as Grades 1–2 by visual detection.



Fig. 11. Damage detection accuracy for a heavily tilted building: (a) the pre-event QuickBird image, (b) the post-event QuickBird image, and (c) a photograph from the ground.

The presence of soft-story damage due to undersized sections, insufficient longitudinal reinforcement, and weak concrete strength was the most common factor observed for the majority of damaged medium-rise buildings during this earthquake. This type of damage, which was generally judged to be between Grades 3 and 4 in the field survey, is difficult to detect from vertical images, including buildings that suffer from severe internal damage. This observation explains why the percentage of incorrectly judged damage for medium-rise buildings with Grades 3 and 4 is high.

Figure 10 shows another example for a 5-story building that was slightly tilted (Grade 4) by the earthquake, with no surrounding debris; it was incorrectly judged as Grades 1–2 by visual detection even when a preevent image was employed as a reference to judge the damage status. Figure 11 shows the same type of building, but heavily tilted and surrounded by debris; the visual detection accuracy for this structure was good even when only the post-event image was used. However,

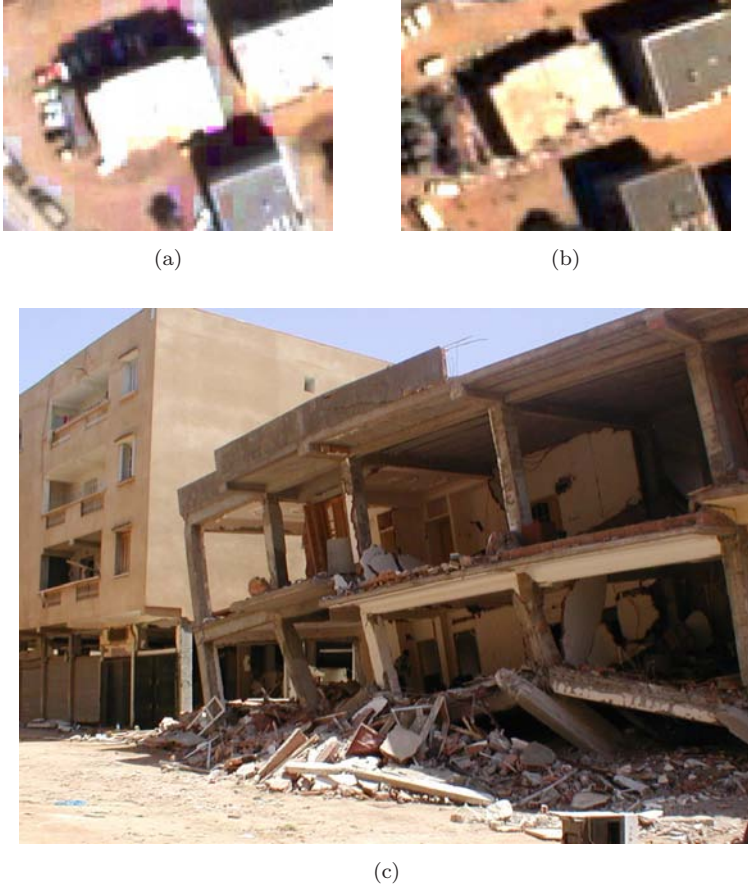


Fig. 12. A case where heavy damage may be difficult to see using only the post-event image; debris surrounding the buildings is hidden by shadow: (a) the preevent QuickBird image, (b) the post-event QuickBird image, and (c) a photograph from the ground.

for some buildings suffering from heavy damage and surrounded by debris, it was difficult to detect damage using only post-event images since the debris was hidden by shadows, as shown in Fig. 12. Studies on the effects of cast-shadows in high-resolution satellite imagery and on the trials to reproduce shadow-free images



Fig. 13. Damage distribution for buildings in Boumerdes city following the 2003 Algeria earthquake. Details for each class are presented in Table 2 according to the nature of damage.

Table 2. Classification of observed damage patterns from field survey: Grades 3–5 are subdivided considering the visual detection accuracy.

Damage	Description
Grade 3–1	Slight damage in columns/beams and walls, the building is surrounded by a few debris
Grade 3–1 (bis)	Slight damage in columns/beams and walls, debris hidden by shadow in the image
Grade 3–2	Slight damage in columns/beams and walls, the building is not surrounded by debris
Grade 4–3	Heavy damage in columns/beams and walls, the building is surrounded by debris
Grade 4–3 (bis)	Heavy damage in columns/beams and walls, debris hidden by shadow in the image
Grade 4–4	Heavy damage in columns/beams and walls, the building is not surrounded by debris; presence of soft-story and slight displacement; the building is slightly tilted; and collapse of short columns
Grade 5–5	Totally collapsed building, surrounded by massive debris
Grades 5–6	Sections of the building collapsed; and the building is heavily tilted
Grades 5–7	First-storey collapse

were carried out by several researchers [Sarabandi *et al.*, 2004; Yamazaki *et al.*, 2009]. But dark cast-shadows by buildings are still not easy to remove.

According to the results of our analysis (Fig. 13), each degree of damage for Grades 3, 4, and 5 is divided into three classes by the nature of damage and visual detection accuracy. Details for each class by the nature of damage is given in Table 2, which presents a summary of results for the relationship between the observed building damage patterns of Grades 3–5 from the field survey and the visual detection accuracy. Figure 14 shows the classification of damage patterns for

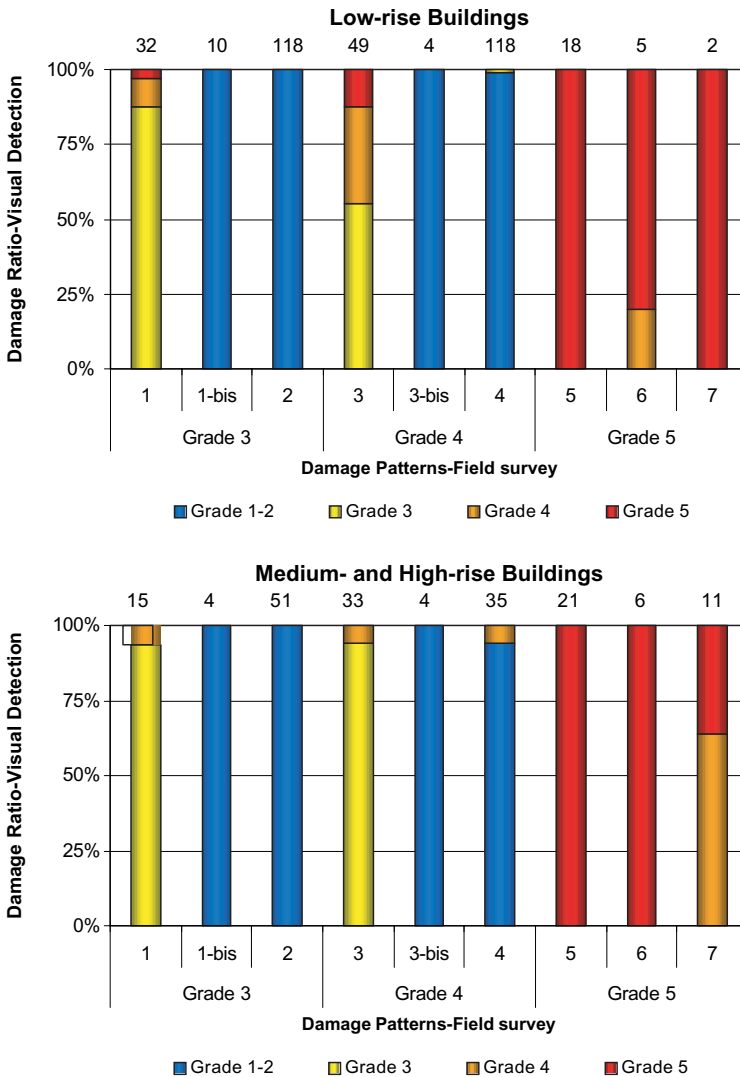


Fig. 14. Accuracy of distinguishing building damage grade from high-resolution satellite imagery, according to damage pattern from field survey.

Grades 3–5 and a comparison with results from the visual detection. For all types of constructions, low-rise as well as medium- and high-rise structures, the nature of observed damage patterns and visualization of debris played a dominant role in damage detection accuracy.

4. Conclusions

Using the QuickBird satellite images of Boumerdes city obtained following the 21 May 2003 Algeria earthquake, we examined the applicability of such high-resolution optical imagery for the visual detection of building damage grades based on ground truth data for the urban nature, building type for 2,794 structures, and the real damage observed. The results are presented as GIS damage mapping, obtained from the QuickBird images and a field survey.

In general, the comparison showed that totally collapsed buildings, partially collapsed buildings, and buildings surrounded by debris can be identified using only post-event high-resolution images. However, due to the nature of damage observed, some heavily damaged buildings were incorrectly identified even when pre-event images were employed as a reference to determine the damage status.

The accuracy of the identified or judged damage grade also depends on the building type (size and height classes) and the urban environment of the zone. There were difficulties in detecting damage for low-rise constructions, especially those located in dense areas. Thus, damage detection from high-resolution optical images is prone to omission errors; hence, it is necessary to consider this fact when estimating damage statistics at an early stage.

Acknowledgments

The QuickBird images used in this study were licensed and provided by the EERI, Oakland, California, USA. The field survey ground dataset was provided by the CGS, Algeria.

References

- Architectural Institute of Japan, Japan Society of Civil Engineers, and The Japan Geotechnical Society. [2001] “Report on the damage investigation of the 1999 Kocaeli earthquake in Turkey,” Maruzen.
- Belazougui, M. [2008] “Boumerdes Algeria earthquake of May 21, 2003: Damage analysis and behavior of beam-column reinforced concrete structures,” *Proc. 14th World Conf. on Earthquake Engineering*, 8 p, Beijing, China, CD-ROM.
- Chirou, L. [2005] “Damage assessment of the 2003 Bam, Iran earthquake using Ikonos imagery,” *Earthquake Spectra* **21**(S1), 219–224.
- Earthquake Engineering Research Institute. [2009] “Reconnaissance forms for field investigations,” <http://www.eeri.org/site/lfe-forms>.
- Eguchi, R. T., Huyck, C. K., Ghosh, S. and Adams, B. J. [2008] “The application of remote sensing technologies for disaster management,” *Proc. 14th World Conf. on Earthquake Engineering*, 8 p, Beijing, China, CD-ROM.

- European Seismological Commission. [1998] *European Seismic Scale 1998*.
- Goretti, A. and Pasquale, G. D. [2004] "Building inspection and damage data for the 2002 Molise, Italy, Earthquake," *Earthquake Spectra* **20**(S1), 167–190.
- Grünthal, G. [2001] European Microseismic Scale 1998, *Cahiers du Centre Européen de Géodynamique et de Séismologie*.
- Hisada, Y., Shibayama, A. and Ghayamghamian, M. R. [2004] "Building damage and seismic intensity in Bam City from the 2003 Iran, Bam, Earthquake," *Bull. Earthquake Res. Inst. Univ. Tokyo*, **79**, 81–93.
- Meslem, A., Yamazaki, F., Maruyama, Y., Benouar, D. and Laouami, N. [2008] "Strong motion distribution and microtremor observation following the 21 May 2003 Boumerdes, Algeria earthquake," *Proc. 14th World Conf. on Earthquake Engineering*, 8 p, Beijing, China, CD-ROM.
- Meslem, A., Yamazaki, F. and Maruyama, Y. [2009] "Evaluation of buildings quality and soil condition in Boumerdes city using damage data following the 2003 Algeria earthquake," In *Safety, Reliability and Risk of Structures, Infrastructures and Engineering Systems*, pp. 3152–3159 (Taylor & Francis).
- Meslem, A., Yamazaki, F., Maruyama, Y., Benouar, D., Laouami, N. and Benkaci, N. "Site-response characteristics evaluated from strong motion records of the 2003 Boumerdes, Algeria earthquake," *Earthquake Spectra* (in press).
- Miura, H. and Midorikawa, S. [2010] "Distribution of building damage areas detected from satellite optical images of the 2006 Central Java, Indonesia, Earthquake," *Proc. 7th International Conf. on Urban Earthquake Engineering*, pp. 229–234.
- Rathje, E. M. and Adams, B. J. [2008] "The role of remote sensing in earthquake science and engineering: Opportunities and challenges," *Earthquake Spectra* **24**(2), 471–492.
- Rathje, E. M., Crawford, M., Woo, K. and Neuenschwander, A. [2005] "Damage patterns from satellite images from the 2003 Bam, Iran earthquake," *Earthquake Spectra* **21**(S1), 295–307.
- Sarabandi, P., Yamazaki, F., Matsuoka, M. and Kiremidjian, A. [2004] "Shadow detection and radiometric restoration in satellite high resolution images," *Proc. IEEE 2004 International Geoscience and Remote Sensing Symposium*, 4 pp, Anchorage, Alaska, CD-ROM.
- Saito, K., Spence, R., Going, C. and Markus, M. [2004] "Using high-resolution satellite images for post-earthquake building damage assessment: A study following the 26 January 2001 Gujarat earthquake," *Earthquake Spectra* **20**(1), 145–169.
- Saito, K., Spence, R. and Foley, T. [2005] "Visual damage assessment using high-resolution satellite images following the 2003 Bam, Iran earthquake," *Earthquake Spectra* **21**(S1), 309–318.
- Yamazaki, F. and Matsuoka, M. [2007] "Remote sensing technologies in post-disaster damage assessment," *J. Earthquake Tsunami* **1**(3), 193–210.
- Yamazaki, F., Kouchi, K., Matsuoka, M., Kohiyama, M. and Muraoka, N. [2004] "Damage detection from high-resolution satellite images for the 2003 Boumerdes, Algeria earthquake," *Proc. 13th World Conf. on Earthquake Engineering*, 13 pp, Vancouver, B.C., Canada, Paper No. 2595.
- Yamazaki, F., Yano, Y. and Matsuoka, M. [2005] "Visual damage interpretation of buildings in Bam city using QuickBird images following the 2003 Bam, Iran earthquake," *Earthquake Spectra* **21**(S1), 329–336.
- Yamazaki, F., Liu, W. and Takasaki, M. [2009] "Characteristics of shadow and removal of its effects for remote sensing imagery," *Proc. IEEE 2009 International Geoscience and Remote Sensing Symposium*, CD-ROM, pp. IV-426–429.